Investigation of Influence of Winding Structure on Reliability of Permanent Magnet Machines

Wei Li, *Member*, *IEEE*, and Ming Cheng, *Fellow*, *IEEE*

***Abstract*—Winding is an important part of the electrical machine and plays a key role in reliability. In this paper, the reliability of multiphase winding structure in permanent magnet machines is evaluated based on the Markov model. The mean time to failure is used to compare the reliability of different windings structure. The mean time to failure of multiphase winding is derived in terms of the underlying parameters. The mean time to failure of winding is affected by the number of phases, the winding failure rate, the fault-tolerant mechanism success probability, and the state transition success probability. The influence of the phase number, winding distribution types, multi three-phase structure, and fault-tolerant mechanism success probability on the winding reliability is investigated. The results of reliability analysis lay the foundation for the reliability design of permanent magnet machines.**

***Index Terms*—phase number, winding distribution, Markov model, reliability, mean time to failure, permanent magnet machine**

I. Introduction

THE permanent magnet (PM) machine has been widely used in the field of electric vehicle, aerospace, rail transportation, offshore wind generation, etc. [1]-[3], due to high efficiency and high-power density. These application fields put forward higher and higher requirements on the performance of the PM machine system, especially the reliability performance is more stringent in continuous operation fields. The winding is an important component of the PM machines. According to the statistics [4], [5], 37% of machine failures are caused by winding. Therefore, the winding reliability is a critical concern in machine applications. The main idea to improve the reliability of winding is to change the phase number and structure of the winding and cooperate with the fault-tolerant algorithm. Thus, multiphase including four-phase, five-phase, six-phase, nine-phase, and twelve-phase PM machines have been investigated [6]-[9]. Moreover, the fault-tolerant control of multiphase PM machine under open-circuit fault was investigated in [10]-[12], including iterative learning control, harmonic current injection, high-frequency current injection, etc. The fault-tolerant control of the dual-winding redundant structure was analyzed in [13]. The redundant winding configuration of the three-phase flux-switching PM (FSPM) machine was analyzed and control strategy for the post-fault operation was proposed in [14]. The fault-tolerant control of nine-phase and twelve-phase FSPM machine under fault was investigated in [15]-[17]. The topology and design of PM fault-tolerant machines were summarized in [18].

It can be seen that the current research is mainly focused on the design of PM machines with redundant structures and fault-tolerant control of PM machines under one or more phase faults. There is lack of quantitative research on the influence of the phase number on reliability and the relationship between machine winding structural and reliability is rarely reported.

The objective of this paper is to investigate the influence of phase number and structure of windings on the reliability based on the Markov model and to establish the relationship between winding structure and machine reliability to lay a foundation for the reliability design of PM machines. This paper is organized as follows. The multiphase winding structure and four kinds of winding distribution are introduced in Section II. The Markov model is presented in Section III. The reliability calculation process is developed in Section IV. The MTTF equation of N-phase machine is calculated by the Markov model in Section V. The relationship between winding structural and machine reliability is analyzed by comparing MTTF in Section V. Finally, conclusions are drawn in Section VII

II. Structure Distribution and Fault of Winding

A. Winding Distribution

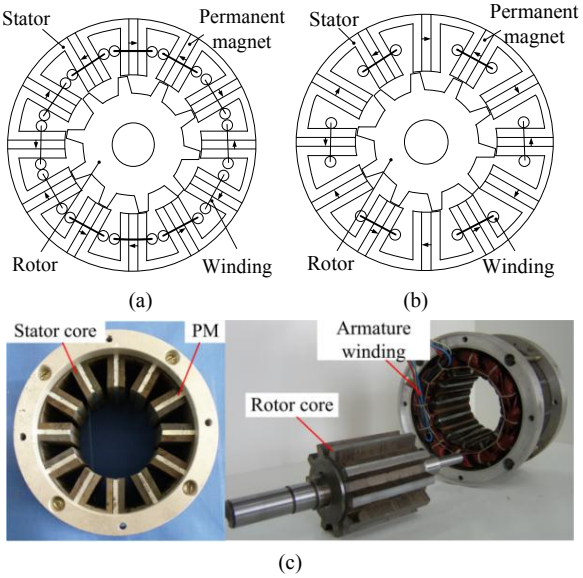

Fig. 1. Schematic diagram of the FSPM machine. (a) CDW (b) CSW (c) Prototype with CDW.

Manuscript was submitted for review on 20, March, 2020.
Wei Li is with Anhui University(e-mail: liwei001x@163.com)
Ming Cheng is with Southeast University(e-mail: mcheng@seu.edu.cn)
Digital Object Identifier 10.30941/CESTEMS.2020.00013

There are four main distribution structures of machine winding, namely distributed single-layer winding (DSW), distributed double-layer winding (DDW), concentrated double winding (CDW), and concentrated single winding (CSW), respectively. The first two distribution structures are mainly used in the rotor-PM machine, and the last two winding distribution structures are mainly used in the stator-PM machine. Fig. 1 shows three-phase FSPM machines with the CDW distribution and CSW distribution respectively. The star connection and delta connection for windings may be used, and the former is chosen to study in this paper.

B. Winding Fault

The machine windings are located in the stator slot. The insulation paper is used for isolation between phases, and also between winding and stator-core. When the performance of the insulation material is degraded, failure may occur. There are three types of winding faults: turn-to-turn short circuit (TTS), phase-to-phase short circuit (PPS) and winding open circuit (WO).

In general, the PPS fault may occur in three locations, which are between the coils in stator slot, between the machine end coils, and between the coils and the coil connection wires. The coil connection wires have special insulation protection, so the PPS fault of the coil connection wires can be neglected. The PPS fault conditions of different winding structures are different. the locations where PPS fault may occur in four different winding distributions are shown in Table I.

TABLE I
POSSIBLE LOCATIONS OF PPS FAULT

Location	DDW	DSW	CDW	CSW
Stator Slot	YES	NO	YES	NO
End Coil	YES	YES	NO	NO

According to the thermodynamic analysis, the highest temperature occurs in the end winding [20], which is, as well known, the most important factor for the life of the insulation material. Therefore, the probability of PPS fault in the end coils is bigger than that in the stator slot. The order of PPS fault in different winding structures is as follows: DDW, DSW, CDW, and CSW. Their reliability comparison is carried out in Section VI.

C. Fault-Tolerant Mechanism

Initially, all windings are in the healthy working state. Each phase winding is connected to the inverter through an auxiliary switch. All auxiliary switches cooperate with some sensors to detect the fault phase, isolate the fault phase and the controller adopts an appropriate fault tolerance algorithm to minimize the fluctuation in the machine performance caused by the fault. This whole process is called the fault-tolerant mechanism (FTM). If the FTM works in time, the machine reliability will increase. If the FTM does not work successfully, the winding faults may become serious and have an inestimable impact on the machine. Therefore, the success probability of FTM should be considered in reliability calculation.

III. MARKOV CALCULATION METHOD

There are many reliability evaluation methods, such as reliability block diagram, Markov method and so on [21]-[23]. The reliability block diagram is a traditional reliability calculation method [21]. The traditional reliability calculation method does not consider the effect of all faults on reliability, so it can't calculate the reliability of multi-state system accurately. The Markov method is another important method for calculating reliability. All states and state transition processes of the system are considered in the Markov model. The next state of system is only associated with the present state, regardless of all previous states [21], [22]. Therefore, the Markov model is used to analyze the multiphase machine in this paper.

The transition probability of machine in this paper is equal to the failure rate of winding which is different in different states. If the system state number is Z, the probability of each state in the Markov chain can be calculated by:

$$\frac{dP_i(t)}{dt} = -\sum_{i\neq j}\lambda_{ij}P_i(t) + \sum_{j\neq i}\lambda_{ji}P_j(t) \tag{1}$$

where $1 \le i, j \le Z$, λ_{ij} represents the rate of the state transitions from state i to j. The collection of all system states is called the state space, $\mathbf{P}(t)=[P_1(t), P_2(t), \dots, P_Z(t)]$. The initial condition of state space is $\mathbf{P}(0)=[1, 0, \dots, 0]$. Also, the collection of all transition probabilities is called the state transition matrix, $\mathbf{\Phi}$. Because the number of the state is S, $\mathbf{\Phi}=(a_{ij})_{Z\times Z}$. The probability of each state can be calculated using the Chapman-Kolmogorov equation [23]:

$$\frac{d\mathbf{P}^{\mathrm{T}}(t)}{dt} = \mathbf{\Phi}^{\mathrm{T}}\mathbf{P}^{\mathrm{T}}(t) \tag{2}$$

where the superscript T represents the transpose of the matrix. The system reliability is equal to 1 subtracting the probability of failure state:

$$R(t) = 1 - P_Z(t) \tag{3}$$

Mean time to failure (MTTF) is an important parameter to judge the reliability, which is defined as the average time that the system can operate, that is:

$$\mathrm{MTTF} = \int_0^\infty R(t)\mathrm{d}t \tag{4}$$

IV. PREMISE OF RELIABILITY ANALYSIS

A. Premise of the Markov Model

A reliable system means that the system meets the working requirements. In other words, even if the system does not fail, the system is not reliable if the system performance does not meet the working requirements. Thus, it is necessary to set a standard in system reliability evaluation. In this paper, 30% value of machine rated torque is set as the reliability standard. It should be noted that this standard value may be changed according to different circumstances.

When TTS fault is slight, it will not affect the reliability of machine [26]. When TTS fault and PPS fault are serious, the windings will burn and break. Therefore, to study the relationship between the number of phase and winding reliability, and simplify the analysis process, the slight TTS fault is not considered in the analysis. The severe TTS fault is approximated as WO fault. The PPS fault can be approximated

as WO fault of two-phase winding.

B. The Failure Rate of Winding

The purpose of this paper is to investigate the relationship between machine winding structure and reliability based on the Markov model. Thus the failure of other components in the machine is not considered. The failure rate of winding is the key parameter to calculate winding reliability. The failure rate model of winding is [24]:

$$\lambda = \lambda_b \pi_T \pi_Q \pi_E \tag{5}$$

where λ_b, π_T, π_Q *and* π_E represent basic failure rate, temperature factor, quality factor, and environmental factor. Assume that λ_b, π_Q *and* π_E of machine winding with different phase numbers are the same. The failure rate of winding is only affected by π_T that is a function of hot spot temperature T_{HS} [24]:

$$\pi_T = e^{\left(\frac{-0.11}{8.617\times10^{-5}}\left(\frac{1}{T_{HS}+273}-\frac{1}{298}\right)\right)} \tag{6}$$

T_{HS} can be calculated by ambient temperature T_A (℃) and temperature rise ΔT (K):

$$T_{HS} = T_A + 1.1\Delta T \tag{7}$$

In the reliability evaluation process, it is assumed that T_A is constant. The most important source of winding temperature is the heat generated by the copper loss. The value of ΔT of winding is mainly related to copper loss.

The key to stable operation of machine is the circular rotating magnetomotive force (MMF) in the air gap. The total magnetic potential of N-phase machine in healthy state is:

$$F = \frac{N}{4} N_S I_m \sin(\omega_e t - \varphi) \tag{8}$$

where N_S, I_m, ω_e, and φ represent the number of turns of per phase winding, the maximum value of phase current, electric angular velocity and electrical angle along air gap.

The copper loss has changed after the fault, so the failure rate of each phase winding in each fault condition is not the same. The failure rate in all states of winding is reflected in state transition matrix $\mathbf{\Phi}$. The reliability equation becomes more and more complex and difficult to solve with the increase of state number. To effectively analyze the reliability of multiphase machine, it is assumed that the winding failure rate is the same in each state.

C. Markov Calculation Process

If one or more phase windings are open-circuited, the amplitude and phase angle of healthy phase currents are adjusted to obtain the same rotating circular MMF as in healthy state based on the principle of constant magnetic potential. The adjusted k-th phase current and MMF after fail can be expressed as:

$$I_k^{'} = I_m(X_k \sin\omega_e t + Y_k \cos\omega_e t) \tag{9}$$

$$\begin{aligned} F^{'} = \frac{N_S I_m}{2}(&\sum X_k \cos\alpha_k \cos\varphi \sin\omega_e t + \sum Y_k \cos\alpha_k \cos\varphi \cos\omega_e t \\ &+ \sum X_k \sin\alpha_k \sin\varphi \sin\omega_e t + \sum Y_k \sin\alpha_k \sin\varphi \cos\omega_e t) \end{aligned} \tag{10}$$

where X_k and Y_k are the coefficients before the sine function and cosine function, and the value of X_k and Y_k are directly related to the amplitude and phase angle of current.

Temperature is the most important factor affecting the winding failure rate. The copper loss ratio before and after the fault is set to:

$$CL = \frac{P_{Cu\_F}}{P_{Cu\_H}} \tag{11}$$

where P_{Cu_F} and P_{Cu_H} represent the copper loss in fault-tolerant and healthy states respectively. In healthy state, the average electromagnetic torque is:

$$T_{em} = \frac{P_{em}}{\omega_r} = \frac{1}{\omega_r}\sum_{k=1}^{N} e_k i_k \tag{12}$$

where P_{em}, e_k, i_k and ω_r represent the electromagnetic power, the back electromotive force (EMF) of k-th phase, the phase current of k-th phase and mechanical angular velocity.

The current amplitude needs to be corrected to ensure the same copper loss before and after the fail. For example, the magnitude of the k-th phase current shown in (9) is corrected to $I_m\sqrt{X_k^2+Y_k^2}\big/\sqrt{CL}$, that is the current amplitude divided by $\sqrt{CL}$. According to (12), the average electromagnetic torque T_{em} is corrected to $T_{em}/\sqrt{CL}$. The corrected torque is compared with the reliability standard to determine whether every state of the system is reliable. Markov chain can be obtained by analyzing all possible fault-tolerant states. At last, the reliability equation or MTTF equation of the machine is calculated according to (2), (3), and (4).

V. Machine Phase and Reliability

A. Relationship between Phase Number and Reliability

The redundancy and fault-tolerant performance of machine gradually increase with the increase of machine phases. In other words, as the phase number increases, the reliability of machine also increases. But there is not a clear quantitative relationship.

If the phase number is N, its Markov chain has N-1 states. The Markov chain of the N-phase machine is shown in Fig. 2. State 1 is healthy state, that is, all phase windings are healthy. State 2 to state N-2 are fault-tolerant state, and the number of fault phases is from 1 to N-3. State F is the failure state, that is, the number of machine health phases is less than 3 or the torque of machine is less than the reliability standard. The transition probability between two states is the product of four parameters: the number of phases that may fail, the failure rate (λ), the success probability of FTM (M) and the success probability of state transition after WO fault (Q) or the success probability of state transition after PPS fault (S).

The meaning that Q and S are not equal to 1 is that the transition success probability between two states is not 100%. That is to say, the all fault-tolerant situations in state i is reliable, but not every condition in state i+1 is reliable. Its unreliable condition may be transferred from state i-1 under PPS fault or state i under WO fault. After obtaining the transition probability among all states, the reliability equation of the N-phase machine can be calculated according to (4) and (5). The transpose of transition matrix $\mathbf{\Phi}$ can be expressed as (13),

where λ_{wo} and λ_{pps} represent the failure rate of WO fault and PPS fault respectively, X_1 to $X_{N\text{-}2}$ represent the number of PPS fault from state 1 to state N-2. The element in $\boldsymbol{\Phi}$ is represented by a_{ij}, which means the probability of transition from state j to state i.

$$\boldsymbol{\Phi}^{\mathrm{T}}=(a_{ij})_{(N-1)(N-1)}=\begin{bmatrix} -(N\lambda_{wo}+X_1\lambda_{pps}) & 0 & \cdots & 0 & \cdots & 0 & 0 \\ N\lambda_{wo}M & -[(N-1)\lambda_{wo}+X_2\lambda_{pps}] & \cdots & 0 & \cdots & 0 & 0 \\ X_1\lambda_{pps}M & [(N-1)\lambda_{wo}]M & \cdots & 0 & \cdots & 0 & 0 \\ 0 & [X_2\lambda_{pps}]M & \cdots & 0 & \cdots & 0 & 0 \\ \cdots & \cdots & \cdots & \cdots & \cdots & \cdots & \cdots \\ 0 & 0 & \cdots & 0 & \cdots & 0 & 0 \\ 0 & 0 & \cdots & -[(N-i+1)\lambda_{wo}+X_i\lambda_{pps}] & \cdots & 0 & 0 \\ 0 & 0 & \cdots & [(N-i+1)\lambda_{wo}]MQ_i & \cdots & 0 & 0 \\ \cdots & \cdots & \cdots & [X_i\lambda_{pps}]MS_i & \cdots & \cdots & \cdots \\ 0 & 0 & \cdots & 0 & \cdots & -3(\lambda_{wo}+X_{N-2}\lambda_{pps}) & 0 \\ (N\lambda_{wo}+X_1\lambda_{pps})(1-M) & [(N-1)\lambda_{wo}+X_2\lambda_{pps}](1-M) & \cdots & [(N-i+1)\lambda_{wo}+X_i\lambda_{pps}]\cdot(1-MQ_i-PS_i) & \cdots & 3(\lambda_{wo}+X_{N-2}\lambda_{pps}) & 0 \end{bmatrix} \tag{13}$$

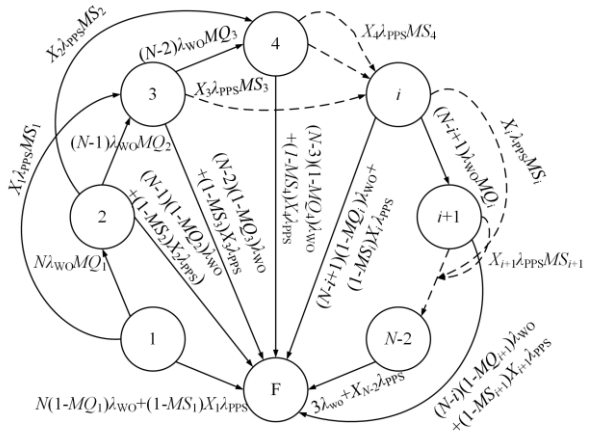

Fig. 2. Markov chain of N-phase machine.

According to (4), (5), and initial conditions, the reliability equation of the N-phase machine can be obtained. This calculation equation is very complex and is not shown here for brevity. According to (6), the MTTF of N-phase machine can be expressed as:

$$\mathrm{MTTF}_N=\mathbf{A}\bullet\mathbf{M} \tag{14}$$

where matrix **A** is the MTTF matrix, matrix **M** is the success probability matrix of FTM. The matrix **A** and the transposition of matrix **M** can be expressed as:

$$\mathbf{A}=\begin{bmatrix} A_{11-0} & 0 & 0 & \cdots & 0 \\ A_{21-0} & A_{21-1} & 0 & \cdots & 0 \\ A_{31-0} & A_{31-1} & A_{31-2} & \cdots & 0 \\ \vdots & \vdots & \vdots & \ddots & \vdots \\ A_{(N-2)1-0} & A_{(N-2)1-1} & A_{(N-2)1-2} & \cdots & A_{(N-2)1-(N-3)} \end{bmatrix} \tag{15}$$

$$\mathbf{M}^{\mathrm{T}}=\begin{bmatrix} 1 & M & M^2 & \cdots & M^{N-3} \end{bmatrix}^{\mathrm{T}} \tag{16}$$

The matrix **A** is lower triangular, and each row vector of the matrix **A** from top to bottom represents state 1 to state N-2. The position of element $A_{i1\text{-}k}$ in **A** is the i-th row and the (k+1)-th column. The meaning of element $A_{i1\text{-}k}$ is that the system takes k steps from state 1 to state i. As shown in Fig. 2, the state transition span at most two states, so $A_{i1\text{-}k}$ equals 0 when (i-1)/k>2.

Take $A_{51\text{-}1}$, $A_{51\text{-}2}$, and $A_{51\text{-}3}$ as examples to illustrate their values. They are in the second column, third column and fourth column of the fifth row in matrix **A**, respectively**.** Their values are as follows:

1) For element $A_{51\text{-}1}$ (i=5, k=1), $(i-1)/k=4>2$, so $A_{51-1}=0$.

2) For element $A_{51\text{-}2}$ (i=5, k=2), $(i-1)/k=2$, so $A_{51-2}\neq 0$. Through the method of permutation and combination, under the premise of spanning two states at most, it is found that there is only one path taking two steps from state 1 to state 5, that is, from state 1 to state 3 and then to state 5. Thus: $A_{51-2}=\left|\dfrac{a_{31}a_{53}}{a_{11}a_{33}a_{55}}\right|$.

where a_{11}, a_{33}, a_{55}, $a_{31,}$ and a_{53} represent the probability of state transition, and their values can be obtained from (13)

3) For element $A_{51\text{-}3}$ (i=5, k=3), $(i-1)/k<2$, so $A_{51-3}\neq 0$. Based on the same principle, there are three paths from state 1 to state 5 in three steps.

Thus: $A_{51-3}=\left|\dfrac{a_{21}a_{42}a_{54}}{a_{11}a_{22}a_{44}a_{55}}+\dfrac{a_{31}a_{43}a_{54}}{a_{11}a_{33}a_{44}a_{55}}+\dfrac{a_{21}a_{32}a_{53}}{a_{11}a_{22}a_{33}a_{55}}\right|$.

According to this rule, the value of all elements in the matrix **A** can be determined quickly. Especially, $A_{11\text{-}0}$ means that the state 1 to the state 1 takes 0 step, which can be derived to be $1/a_{11}$. The other elements that k equals 0 are unlikely to succeed, so the value of these elements is 0. After determining the rule of all the elements, the MTTF of all windings can be quickly calculated by the computer. It is worth noting that (16) has got rid of the complex calculation process of the differential equation in (4), and can easily derive the matrix **A** after knowing the value of each element in the matrix **Φ**. And the above-mentioned rule for determining the matrix **A** is universal, that is to say when the Markov chain shown in Fig. 2 changes, matrix **A** can be determined quickly according to this rule. The MTTF in each state can be quickly known through this matrix, and the influence of state transition rate on MTTF can be obtained.

B. Example

Taking the six-phase machine with CDW winding structure in [25] as an example to illustrate the use of (16).

Six-phase machine winding has three fault types and subdivided into seven fault-tolerant conditions, as shown in Fig. 3, where dotted line and solid line represent fail phase and healthy phase, respectively.

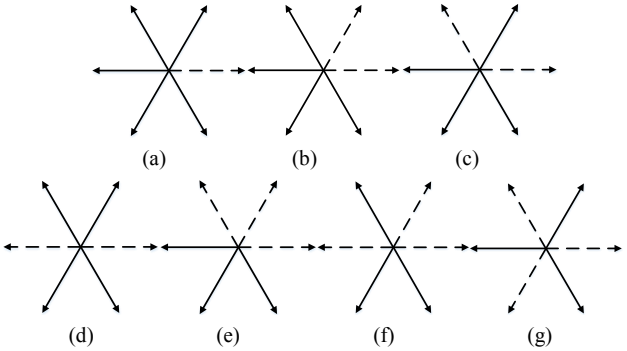

Fig. 3. Fault-Tolerant conditions of the six-phase machine

After the winding faults, the minimum copper loss (MCL) method is used to calculate the healthy phase current [13]. The value of current amplitude (CA) and current phase angle (CPA) for the seven fault-tolerant conditions in Fig. 3 are listed in Table II.

TABLE II
SIX-PHASE CURRENT AMPLITUDE AND PHASE ANGLE IN FAULT-TOLERANT STATE

		A	B	C	D	E	F
(a)	CA	F	$1.453I_m$	I_m	$1.333I_m$	I_m	$1.453I_m$
	CPA	F	-36.58	-120	180	120	36.58
(b)	CA	F	F	$2.107I_m$	$1.833I_m$	$1.833I_m$	$2.107I_m$
	CPA	F	F	-64.71	169.12	130.89	4.71
(c)	CA	F	$1.666I_m$	F	$1.764I_m$	I_m	$1.764I_m$
	CPA	F	-60	F	-60.91	120	40.91
(d)	CA	F	$1.732I_m$	$1.732I_m$	F	$1.732I_m$	$1.732I_m$
	CPA	F	-30	-150	F	150	30
(e)	CA	F	F	F	$3.464I_m$	$6I_m$	$3.464I_m$
	CPA	F	F	F	-90	120	-30
(f)	CA	F	F	$1.732I_m$	F	$3I_m$	$3.464I_m$
	CPA	F	F	-90	F	180	30
(g)	CA	F	$2I_m$	F	$2I_m$	F	$2I_m$
	CPA	F	-60	F	-180	F	60

If the copper loss of all states is the same, the machine torque in all fault-tolerant states drops to 86.61%, 62.02%, 77.46%, 70.71%, 31.62%, 50% and 70.71% of that in the healthy state, respectively. These values satisfy the reliability standard, namely 30%, so all fault-tolerant states are reliable. Thus, the values of Q and S are 1. The Markov chain of the six-phase machine is illustrated in Fig. 4.

The matrix $\mathbf{\Phi}$ can be constructed according to (13) and Fig. 4. The matrix $\mathbf{A}$ can be constructed according to (15). The MTTF equation of the six-phase machine with CDW winding structure is:

$$\begin{aligned}\mathrm{MTTF}_{6p} = &\frac{1}{6\lambda_{wo}+6\lambda_{pps}}+\frac{6\lambda_{wo}M}{(6\lambda_{wo}+6\lambda_{pps})(5\lambda_{wo}+4\lambda_{pps})}\\&+\frac{6\lambda_{pps}M}{(6\lambda_{wo}+6\lambda_{pps})(4\lambda_{wo}+2.4\lambda_{pps})}\\&+\frac{30\lambda_{wo}^2M^2}{(6\lambda_{wo}+6\lambda_{pps})(5\lambda_{wo}+4\lambda_{pps})(4\lambda_{wo}+2.4\lambda_{pps})}\\&+\frac{24\lambda_{wo}\lambda_{pps}M^2}{(6\lambda_{wo}+6\lambda_{pps})(4\lambda_{wo}+2.4\lambda_{pps})(3\lambda_{wo}+1.3\lambda_{pps})}\end{aligned} \tag{17}$$

$$+\frac{24\lambda_{wo}\lambda_{pps}M^2}{(6\lambda_{wo}+6\lambda_{pps})(5\lambda_{wo}+4\lambda_{pps})(3\lambda_{wo}+1.3\lambda_{pps})}$$
$$+\frac{120\lambda_{wo}^3M^3}{(6\lambda_{wo}+6\lambda_{pps})(5\lambda_{wo}+4\lambda_{pps})(4\lambda_{wo}+2.4\lambda_{pps})(3\lambda_{wo}+1.3\lambda_{pps})}$$

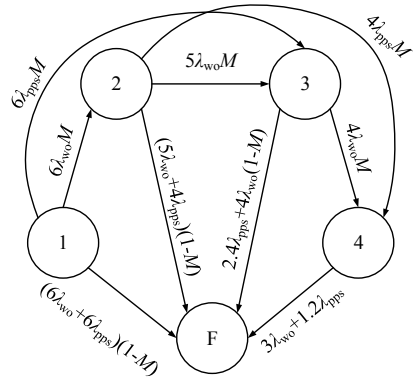

Fig. 4. Markov chain of six-phase machine.

VI. RELIABILITY COMPARISON

In the previous section, the MTTF equation of N-phase machine is derived, and the meaning of each element in matrix $\mathbf{A}$ is explained in detail. Finally, the six-phase machine with CDW structure is taken as an example. In this section, the effects of different winding structures, machine phase numbers, failure rate, and the FTM success probability on MTTF are investigated.

A. Winding Structure

In Section II, the locations of DDW, DSW, CDW, and CSW structures where PPS fault may occur are discussed. In the end winding, the PPS fault may occur between each phase. In the stator slot, the PPS fault can occur only in two adjacent phases. The sum of the number of PPS fault at these two locations equal to the coefficients X_1 to X_{N-2} in the matrix $\mathbf{\Phi}$. Because of the PPS fault only occur in the stator slots for CDW structure. The coefficients X_1 to X_{N-2} are equal to the number of PPS fault that may occur in the stator slots under different states.

1) In State 1, the two adjacent phases will have PPS fault, so there are six types of PPS fault, X_1=6.

2) In State 2, one phase has a WO fault, so there are four types of PPS fault in the five healthy phases, X_2=4.

3) In State 3, WO fault occurs in two phases, so there are three tolerant-fault conditions: adjacent two phases fault, one phase, and two phases interval between two fault phases. These are 3, 2, and 2 types of PPS fault in the three tolerant-fault conditions. X_3 is equal to 2.4, which is the average number of PPS fault types.

4) In State 4, WO fault occurs in three phases, so there are 0 or 2 or 3 kinds of PPS fault in the three healthy phases. The value of X_4 is also equal to the average number of PPS fault types, which is equal to 1.3.

After determining the coefficient problem before λ_{pps}, the reliability of these four structures is compared. To ensure a fair comparison, the FTM success probability is set to 100% (M=1). Their MTTF equations of six-phase winding are calculated by using the above method. The detailed equations are not shown

here due to space limitation, but they are functions made up of λ_{wo} and λ_{pps}. The MTTF surfaces of these four winding structures are drawn for comparison as shown in Fig. 5. It is clear from the figure that the reliability sequence from high to low is CSW, CDW, DSW, and DDW structure. The gap between them increases with the decrease of λ_{pps} and λ_{wo}, especially λ_{wo}.

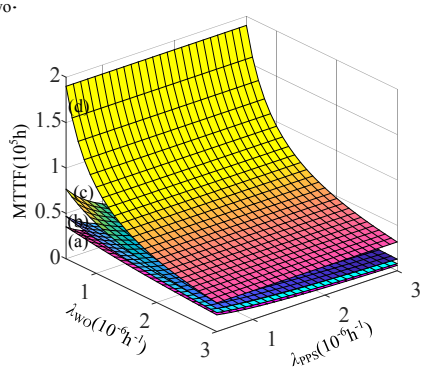

Fig. 5. MTTF surfaces of different winding distributions with λ_{WO} and λ_{PPS} (a) DDW distribution (b) DSW distribution (c) CDW distribution (d) CSW distribution.

The partial differential of MTTF equations of DDW, DSW, CDW, and CSW structures are performed for λ_{wo} and λ_{pps} respectively by equation (18).

$$\Delta\text{MTTF}=\left|\frac{\partial\text{MTTF}}{\partial\lambda_{wo}}\right|-\left|\frac{\partial\text{MTTF}}{\partial\lambda_{pps}}\right| \tag{18}$$

The CSW structure does not cause PPS fault, so its MTTF is only affected by WO fault. For CDW structure, the result of (18) is less than 0 only when λ_{wo} is about 100fit. λ_{wo} reaches this value is a serious challenge under complex conditions, and its range is very small. So, in general, the impact of WO fault on MTTF is greater than that of PPS fault on MTTF for centralized winding structure. For DSW and DDW structures, the results of (21) are less than 0. So, the effect of PPS fault on MTTF is greater than that of WO fault on MTTF.

Therefore, appropriate methods are adopted to reduce the value of λ_{wo} and λ_{pps} to improve the reliability of the winding, thereby improving the reliability of the machine. Obviously, the PPS fault needs to be prioritized for distributed winding and the WO fault needs to be prioritized for concentrated winding.

B. Machine Phase Number

The CSW structure is only related to λ_{wo}, so the reliability of the CSW structure is proportional to the number of phases. The influence of λ_{wo} and λ_{pps} on MTTF should be considered in CDW, DSW and DDW structures. Taking three-phase, four-phase, five-phase, six-phase, and nine-phase DSW structures as examples, their MTTF surfaces are drawn which are illustrated in Fig. 6.

All MTTF surfaces decrease with the increase of λ_{wo} and λ_{pps}. Because the PPS fault has a greater impact on MTTF, the rate of decrease of the MTTF surface on the λ_{pps} side is greater than the rate of decrease on the λ_{wo} side, which also confirms the analysis of (18). The all MTTF surfaces in Fig. 6 intersect each other.

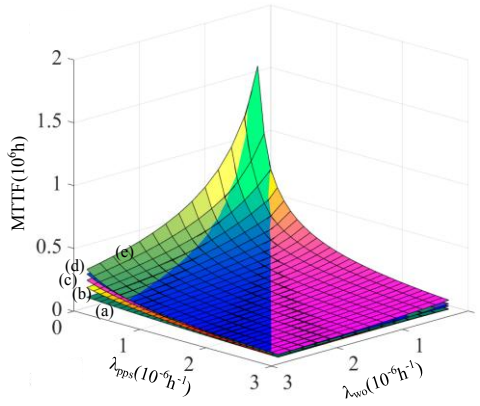

Fig. 6. MTTF surfaces of DSW winding structure (a) three-phase winding (b) four-phase winding (c) five-phase winding (d) six-phase winding (e) nine-phase winding.

To analyze the change of MTTF more clearly, the MTTF surface is simplified into a plane curve. Three values of λ_{wo} and λ_{pps} are selected to get six figures, as shown in Fig. 7.

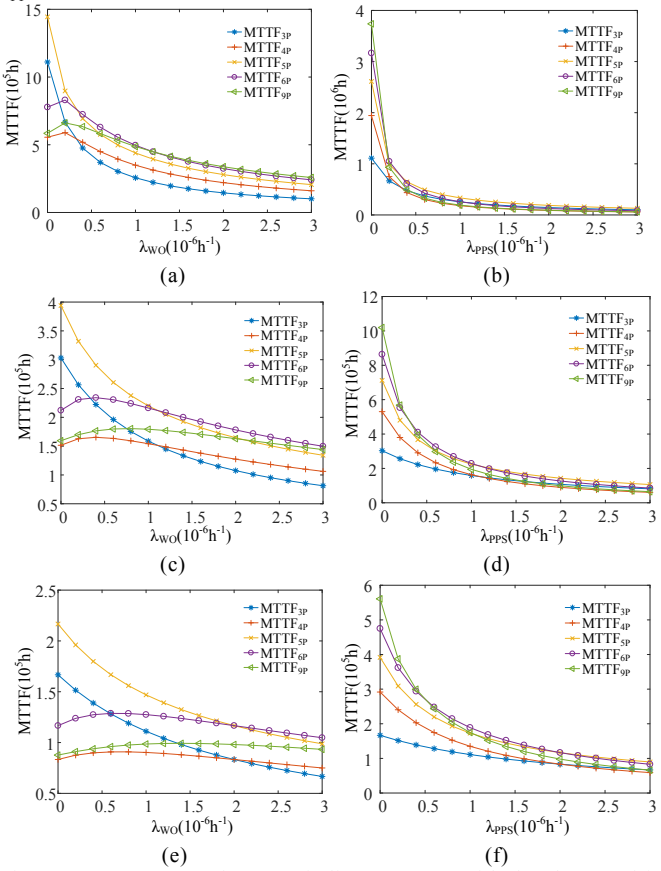

Fig. 7. MTTF curves of DSW winding structure with the change of λ_{wo} and λ_{pps} (a) λ_{pps}=300FIT (b) λ_{wo}=300FIT (c)λ_{pps}=1100FIT (d) λ_{wo}=1100FIT (e) λ_{pps}=2000FIT (f) λ_{wo}=2000FIT.

It can be seen from Fig. 6 and Fig. 7 that the MTTF of the five-phase winding and the six-phase winding are the same when λ_{wo} and λ_{pps} are the same. The MTTF of the five-phase winding is the largest when λ_{wo} is less than λ_{pps}, and the difference between the MTTF of five-phase windings and that of other windings increases with the increase of the difference between λ_{wo} and λ_{pps}. On the contrary, the MTTF of six-phase winding is the greatest when λ_{wo} is greater than λ_{pps}, but the MTTF of nine-phase winding will exceed that of six-phase

winding with the increase of the difference between λ_{wo} and λ_{pps}. Therefore, when λ_{wo} is greater than λ_{pps}, the machine phase number is selected according to λ_{wo} and λ_{pps} and the difference between them.

After analyzing the four winding structures, it was found that the MTTF is affected by two parameters, λ_{wo} and λ_{pps}. They play an important role in the selection of machine phases for the distributed winding structure. For concentrated winding structure, the greater the number of phases, the greater the reliability and the higher the cost.

C. Multi-Three Phase Machine

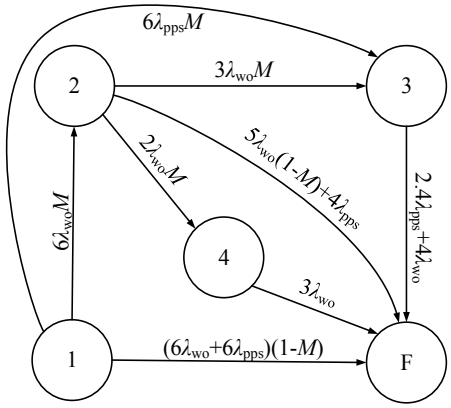

Fig. 8. Markov chain of double three-phase machine.

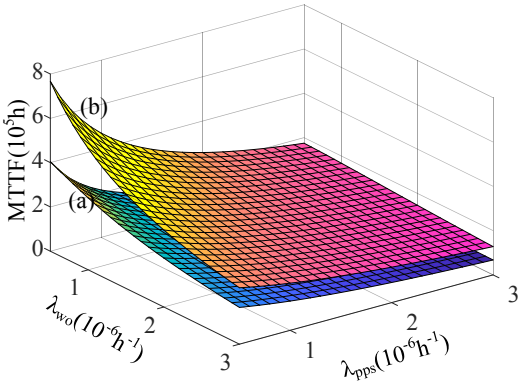

Fig. 9. MTTF surface of six-phase winding and double three-phase winding (a) double three-phase winding (b) six-phase winding.

When the phase number of multiphase machine can be divided by three, the multiphase machine can be regarded as a combination of multi three-phase machine. For example, six-phase and nine-phase can be considered as double three-phase and triple three-phase. In this kind of winding structure, one group three-phase winding needs to be removed when two faults occur in the same group winding.

When the six-phase winding shown in Fig. 4 adopts double three-phase structure [28], its Markov chain is illustrated in Fig. 8. The meaning of each state in Fig. 8 is the same as that in Fig. 4. State 3 indicates that one phase winding of each group three-phase winding has failed. State 4 indicates that one group winding is healthy and the other group is removed. If any phase fails in these two states, the system will fail, so there is no state transfer between them. When a PPS fault occurs in a group winding, this group winding also needs to be removed, so the machine state can be directly transferred from state 1 to state 4. In state 4, the healthy three-phase windings are not adjacent with each other in the stator slots, so PPS fault is unlikely to occur. According to (13), (14) and Fig. 8, the MTTF equation of double three-phase winding can be derived as:

$$\begin{aligned} MTTF_{3p} &= \frac{1}{6\lambda_{wo}+6\lambda_{pps}} \\ &+ \frac{10\lambda_{wo}M}{(5\lambda_{wo}+4\lambda_{pps})(6\lambda_{wo}+6\lambda_{pps})} \\ &+ \frac{6\lambda_{pps}M}{(4\lambda_{wo}+2.4\lambda_{pps})(6\lambda_{wo}+6\lambda_{pps})} \\ &+ \frac{18\lambda_{wo}^2M^2}{(4\lambda_{wo}+2.4\lambda_{pps})(5\lambda_{wo}+4\lambda_{pps})(6\lambda_{wo}+6\lambda_{pps})} \end{aligned} \tag{19}$$

Comparing the MTTF of six-phase and double three-phase winding, as shown in Fig. 9, the double three-phase winding offers lower MTTF than the six-phase winding within the range shown in the figure.

D. FTM success probability

The previous analysis is based on the situation that the value of M is 1, which is not the case in practical applications. Here, the influence of the value of M on the reliability of the winding is analyzed. The curves of the MTTF of the three-phase to nine-phase DSW winding change with M as shown in Fig. 10 when λ_{wo} and λ_{pps} are constant. With the decrease of M, the MTTF curves decrease gradually except three-phase winding, and the MTTF sequence changes.

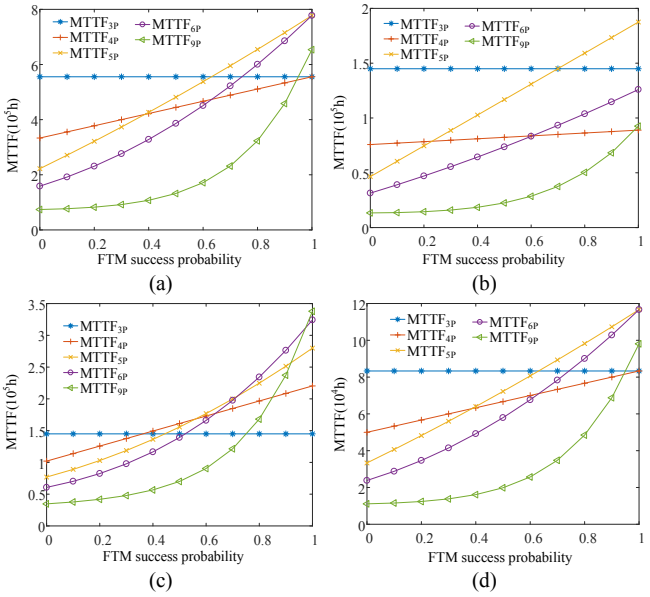

Fig. 10. MTTF varying with FTM success probability(M) (a) λ_{pps}=300FIT, λ_{wo}=300FIT (b) λ_{pps}=2000FIT, λ_{wo}=300FIT (c) λ_{pps}=300FIT, λ_{wo}=2000FIT (d) λ_{pps}=2000FIT, λ_{wo}=2000FIT.

It is known from (a), (b) and (d) that when λ_{wo} and λ_{pps} are equal or λ_{wo} is less than λ_{pps}, the MTTF of the five-phase winding is the largest, and the MTTF sequence is not affected by M in a large range. When λ_{wo} is greater than λ_{pps}, the MTTF sequence is susceptible to M. The same method is used to analyze CDW. The MTTF varying with M not shown here due to space limitation. The MTTF of nine-phase winding is the largest and the ranking is not affected by M in a large range. The second and third places of MTTF sequence are susceptible

when λ_{wo} is less than λ_{pps}.

VII. Simulation and Experimental

In the previous studies, every fault-tolerant state is Markov chain is determined based on the MCL control strategy based on keeping the rotating MMF the same. The accuracy of all states can be determined by verifying the fault-tolerant method.

In order to validate the phase current performance after open-circuit fault, a 20-stator-slot/18-rotor-pole five-phase FSPM machine simulation model and experiment platform are establish. The simulation model is built by the mathematical model and established in MATLAB/Simulink, as illustrated in Fig. 11. The ideal switch is used to simulate the open-circuit fault of the winding in the simulation.

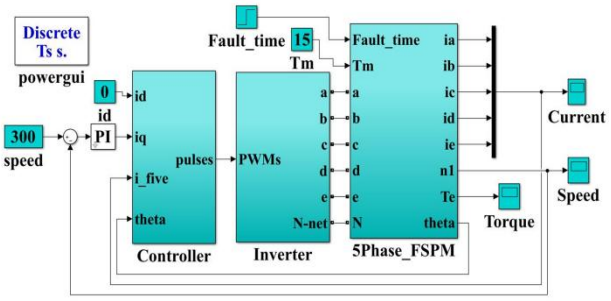

Fig. 11. Five-phase FSPM machine simulation model.

The experiment platform is established as illustrated in Fig. 12, where a dSPACE is used to control the FSPM machine. A magnetic powder brake is used as a load in this experiment platform. A torque transducer is connected between the FSPM machine and load to measure real-time torque. The real-time winding current is measured by the current clamp.

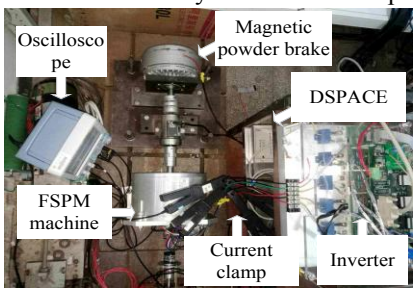

Fig. 12. The experiment platform of FSPM machine.

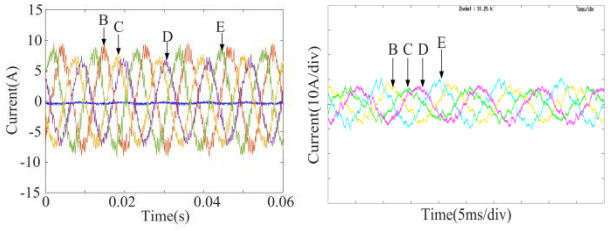

(a) (b)

Fig. 13. Current waveform in fault-tolerant state when Phase A is open-circuit (a) Simulation result (b) Experimental result.

When the load of this five-phase FSPM machine is 15N·m, the current simulation waveform of the Phase A open-circuit fault is shown in Fig. 13 (a), and Fig. 13 (b) is the experimental result. Comparing Fig. 13 (a) and (b), the simulation and experiment current waveforms are basically the same, which proves the accuracy of the fault-tolerant method in reliability analysis.

VIII. Conclusion

In this paper, the relationship between multiphase winding structural and machine reliability has been investigated based on Markov model. The MTTF matrix of *N*-phase winding has been developed to quickly calculate the MTTF of winding. The MTTF of DDW, DSW, CDW and CSW distribution structures have been analyzed and compared, of which the CSW is found to be the best. Three-phase, four-phase, five-phase, six-phase and nine-phase winding are analyzed and their MTTF equations are calculated and compared. For concentrated winding, the more phases, the higher reliability. At the same time, the cost of machine will increase with the increase of phase number. For distributed winding, the reliability of windings is not only related to the phase number, but also the failure rate of different faults. The influence of FTM is also considered in the state transition. It affects the reliability of multiphase winding together with the winding failure rate. The reliability of multi three-phase winding is lower than that of the same phase winding. Therefore, the selection of machine phase number and winding distribution needs to be considered comprehensively according to different application environments, cost, and failure rate.

References

[1] M. Cheng, L. Sun, G. Buja, L. Song, "Advanced electrical machines and machine-based systems for electric and hybrid vehicles," *Energies.* vol. 8, no. 9, pp. 9541-9564, Sept. 2015.

[2] M. Villani, M Tursini, G. Fabri, L. Castellini, "High reliability permanent magnet brushless motor drive for aircraft application," *IEEE Trans. Ind. Electron.*, vol. 59, no. 5, pp. 2073–2081, May 2012.

[3] M. Cheng, Y. Zhu, "The state of the art of wind energy conversion systems and technologies: A review," *Energy Convers. Manage.*, vol. 88, pp. 332–347, Dec. 2014.

[4] M. Cheng, J. Hang, J. Zhang, "Overview of fault diagnosis theory and method for permanent magnet machine," *Chinese Journal of Electrical Engineering,* vol. 1, no. 1, pp. 21-36, Dec. 2015.

[5] R.C. Gleichman, "Failure modes and field testing of medium-voltage motor windings," *IEEE Trans. on Ind. Appl.*, vol. 38, no. 5, pp. 1473-1476, Sept./Oct. 2002.

[6] X. Xue, W. Zhao, J. Zhu, G. Liu, X. Zhu, M. Cheng, "Design of five-Phase modular flux-Switching permanent-magnet machines for high reliability applications," *IEEE Trans. on Magn.*, vol. 49, no. 7, pp. 3941-3944, July 2013.

[7] G. Zhang, W. Hua, M. Cheng, J. Liao, "Design and comparison of two six-phase hybrid-excited flux-switching machines for EV/HEV applications," *IEEE Trans. on Ind. Electron.*, vol. 63, no. 1, pp. 481-493, Jan. 2016.

[8] F. Li, W. Hua, M. Tong, G. Zhao, M. Cheng, "nine-phase flux-switching permanent magnet brushless machine for low-speed and high-torque applications," *IEEE Trans. on Magn.*, vol. 51, no. 3, pp. 8700204, Mar. 2015.

[9] L. Shao, W. Hua, N. Dai, M. Tong, M. Cheng, "Mathematical modeling of a 12-phase flux-switching permanent-magnet machine for wind power generation," *IEEE Trans. on Ind. Electron.*, vol. 63, no. 1, pp. 504-516,

[10] F. Li, W. Hua, M. Cheng, G. Zhang. "Analysis of fault tolerant control for a nine-phase flux-switching permanent magnet machine," *IEEE Trans. Magn.*, vol. 50, no. 11, pp. 8206004, Nov. 2014.

[11] A. S. Thomas, Z. Q. Zhu, Richard L. Owen, Geraint W. Jewell, and David Howe, "Multiphase flux-switching permanent-magnet brushless machine for aerospace application," *IEEE Trans. Ind. Appl.*, vol. 45, no. 6, pp. 1971-1981, Nov.-Dec. 2009.

[12] G. Liu, M. Chen, W. Zhao, Q. Chen, W. Zhao, "Design and analysis of five-phase fault-tolerant interior permanent-magnet vernier machine," *IEEE Trans. on Appl. Supercon.*, vol. 26, no. 4, pp. 0604805, Jun. 2016.

[13] F. Yu, M. Cheng, K. T. Chau. "Controllability and performance of a nine-phase FSPM machine under severe five open-phase fault conditions," *IEEE Trans. Energy Conver.*, vol. 31, no. 1, pp. 323-332, March 2016.

[14] W. Zhao, M. Cheng, W. Hua, H, Jia, R. Cao, "Back-EMF harmonic analysis and fault-tolerant control of flux-switching permanent-magnet machine with redundancy," *IEEE Trans. Ind. Electron.*, vol. 58, no. 5, pp. 1926-1935, May 2011.

[15] J. Hang, J. Zhang; S. Ding; M. Cheng, "Fault diagnosis of high-resistance connection in a nine-phase flux-switching permanent-magnet machine considering the Neutral-Point Connection Model," *IEEE Trans. Power Electron.*, vol. 32, no. 8, pp. 6444-6454. Aug. 2017.

[16] T. Raminosoa, C. Gerada, "Fault tolerant winding technology comparison for flux switching machine," in *Proc. International Conference on Electrical Machines,* Rome, 2010, pp. 1-6.

[17] L. Shao, W. Hua, Z. Q. Zhu, M. Tong, G. Zhao, F.Yin, Z. Wu, M. Cheng, "Influence of rotor-pole number on electromagnetic performance in 12-phase redundant switched flux permanent magnet machines for wind power generation," *IEEE Trans. on Ind. Appl.*, vol. 53, no. 4, pp. 3305-3316, Jan. 2017.

[18] W. Zhao, L. Xu, G. Liu, "Overview of permanent-magnet fault-tolerant machines: topology and design," *CES Transactions on Electrical Machines and Systems*, vol. 2, no. 1, pp. 51-64, Mar. 2018.

[19] X. Jiang, W. Huang, R. Cao, Z. Hao, J. Li, W. Jiang, "Analysis of a dual-winding fault-Tolerant permanent magnet machine drive for aerospace applications," *IEEE Trans. on Magn.,* vol. 51, no. 11, pp. 8114704, Nov. 2015.

[20] N. Arbab, W. Wang, C. Lin, J. Hearron, B. Fahimi, "Thermal modeling and analysis of a double-dtator dwitched reluctance motor," *IEEE Trans. on Energy Conver.*, vol. 30, no. 3, pp. 1209-1217, Sept. 2015.

[21] M. Rausand and A. Hoyland, *System Reliability Theory: Models, Statistical Methods and Applications*, 2nd ed. Hoboken, NJ: Wiley, 2005.

[22] I. B. Gertsbakh, Y. Shpungin, *Models of Network Reliability: Analysis, Combinatorics, and Monte Carlo*, USA: CRC Press, 2010.

[23] A. M. Bazzi, Alejandro Dominguez-Garcia and Philip T. Krein, "Markov reliability modeling for induction motor drives under field-oriented control," *IEEE Trans. Ind. Electron.*, vol. 27, no. 2, pp. 534-546, Feb. 2012.

[24] *Military Handbook Reliability Prediction of Electronics Equipment*, US Department of Defense, MIL-HDBK-217 F, 1995.

[25] G. Zhang, W. Hua, P. Han, "Quantitative evaluation of the topologies and electromagnetic performances of dual-three-phase flux-switching machines," *IEEE Trans. on Ind. Electron*., vol. 65, no. 11, pp. 9157-9167, Nov. 2018.

[26] W. Li, M. Cheng, "Reliability analysis and evaluation for flux-switching permanent magnet machine," *IEEE Trans. Ind. Electron.*, vol. 66, no. 3, pp. 1760-1769, Mar. 2019.

[27] M. Tursini, M. Villani, A. D. Tullio, etc., "Nonlinear model suitable for the offline cosimulation of fault-tolerant PM motors drives," *IEEE Trans. On Ind. Appl.*, vol. 53, no. 4, pp. 3719-3729. July/Aug. 2017.

[28] M. Taha, J. Wale, D. Greenwood, etc., "Design of a high power-low voltage multiphase permanent magnet flux switching machine for automotive applications," in *Proc. IEEE International Conference Electric Machines and Drives Conference,* Miami, 2017, pp. 17083807.

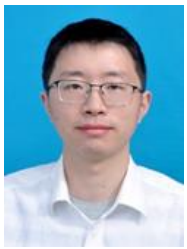

Wei Li (M'13) was born in Anhui, China, in 1986. He received the B.Sc.degree from Anhui University of Technology, Ma'anshan, China, in 2008, the M.E. degree from Anhui University, Hefei, China, in 2012, and the Ph.D degrees from the School of Electrical Engineering, Southeast University, Nanjing, China, in 2019.

Since 2017, he has been with Anhui University, Hefei, China. His current research interests include the reliability of permanent magnet machines for application in hybrid vehicles.

Ming Cheng (M'01–SM'02–F'15) received the B.Sc. and M.Sc. degrees from the Department of Electrical Engineering, Southeast University, Nanjing, China, in 1982 and 1987, respectively, and the Ph.D. degree from the Department of Electrical and Electronic Engineering, The University of Hong Kong, Hong Kong, in 2001, all in electrical engineering.

Since 1987, he has been with Southeast University, where he is currently a Chair Professor with the School of Electrical Engineering and the Director of the Research Center for Wind Power Generation. From January to April 2011, he was a Visiting Professor with the Wisconsin Electric Machine and Power Electronics Consortium, University of Wisconsin, Madison, WI, USA. He has authored or coauthored more than 400 technical papers and 4 books, and is the holder of 120 patents in these areas. His teaching and research interests include electrical machines, motor drives for EV, and renewable energy generation.

Prof. Cheng is a Fellow of the Institution of Engineering and Technology. He has served as the Chair and an Organizing Committee Member for many international conferences. He was a Distinguished Lecturer of the IEEE Industry Application Society for 2015/2016.